Paramagnetic point defects in boron-implanted $Hg_{0.7}Cd_{0.3}Te$ and CdTe

R. C. Bowman, Jr.
Chemistry and Physics Laboratory, The Aerospace Corporation, Los Angeles, California 90009

E. L. Venturini
Sandia National Laboratories, Albuquerque, New Mexico 87185

S. N. Witt
Division of Chemistry and Chemical Engineering, California Institute of Technology, Pasadena, California 91125

(Received 5 November 1986; accepted 15 April 1987)

This paper describes the initial observations of electron paramagnetic resonance (EPR) spectra from $Hg_{0.7}Cd_{0.3}Te$ and CdTe after implantation with boron ions. Sharp and nearly isotropic EPR signals with the free-electron g values were easily detected at low temperatures (i.e., $\leqslant 78$ K) when the boron ion implant dose was 1×10^{16} ions/cm^2 or larger. For identical implant conditions, more intense signals and narrower peaks were obtained from $Hg_{0.7}Cd_{0.3}Te$ samples when compared to the spectra for CdTe. However, the g factors for all implanted $Hg_{1-x}Cd_xTe$ samples appear to be equivalent and are very similar to the values reported for the dangling-bond defects in other ion-implanted semiconductors. The EPR spectra produced by the boron implants do not seem to correspond to either the degenerate conduction electron bands that form in ion-implanted $Hg_{1-x}Cd_xTe$ or the shallow donor states previously found in chemically doped CdTe. When implanted crystals are cooled below 4 K, partially resolved two-component line shapes are observed at some orientations. Increasing temperature causes these two-component lines to collapse into nearly Lorentzian line shapes with temperature-dependent widths. This behavior is consistent with a thermally activated process by which the paramagnetic spins hop between inequivalent locations.

I. INTRODUCTION

Ion implants are commonly utilized during the fabrication of $Hg_{1-x}Cd_xTe$ infrared–photodiode devices. Without further processing, these implants always appear[1–3] to create an n-type layer in $Hg_{1-x}Cd_xTe$. While the nature of these donor states has not been definitively established, they are widely believed[1–3] to be implant-induced damage "defects" and not the implanted atoms. However, thermal anneals can electrically activate some implanted species to show[3] donor (e.g., In) or acceptor (e.g., P) behavior. The properties of implanted boron atoms, which should be donors when substituted on the metal sites in $Hg_{1-x}Cd_xTe$, remains very controversial. Although it is unclear[2,3] whether the implanted boron ions play any direct role as active donors in the formation of the n–p junction, boron implants have been widely used[1] to produce photodiodes. More complete information on their interactions with damage defects or impurities is needed to resolve the specific contributions of boron atoms to the electrical properties of implanted $Hg_{1-x}Cd_xTe$.

Electron paramagnetic resonance (EPR) spectroscopy, which is also known as electron spin resonance (ESR), is a very powerful method to characterize point defects in elemental and compound semiconductors. Analyses of the experimental EPR parameters such as the g-factor constant, fine-structure constant, and hyperfine coefficients can unequivocally identify paramagnetic defects or impurities in many instances.[4] Although EPR studies have been performed on numerous II–VI compound semiconductors,[5–7] relatively few results are available for the $Hg_{1-x}Cd_xTe$ system. While characteristic EPR spectra have been reported for transition metals,[8] shallow donors,[9] and deep donors,[10,11] in CdTe, only two papers[12,13] have presented EPR results for the ternary $Hg_{1-x}Cd_xTe$ alloys. Consequently, EPR experiments have been performed on boron-implanted CdTe and $Hg_{0.7}Cd_{0.3}Te$ crystals to determine whether donor states or other paramagnetic species have been created by the implantation process. In fact, rather intense EPR signals with "free-electron" spin characteristics have been detected at low temperatures following boron implants of 10^{16} ions/cm^2 or larger. Although the specific defects responsible for this new signal cannot yet be identified, the spectral properties are very similar to the EPR spectra for the dangling-bond centers previously found in ion implanted silicon[14] and GaP.[15] Thermal anneals up to 300 °C do not significantly alter the concentration of the paramagnetic defects in boron-implanted $Hg_{1-x}Cd_xTe$ although some minor changes in the EPR spectra are apparent.

II. EXPERIMENTAL BACKGROUND

Two X-band (i.e., nominal resonant microwave frequency of 9 GHz) spectrometers were used for the EPR measurements. A Varian E-line spectrometer has a slotted window in one wall of the microwave cavity which permitted *in situ* illumination of samples at temperatures down to about 5 K when used with an Air Products Heli–Tran liquid transfer system. A second home-built homodyne spectrometer with the microwave cavity in a cold helium gas flow permitted in-dark EPR measurements at temperatures as low as 2 K. Prior calibrations of this latter spectrometer provided accurate g-value determinations as well as estimates of the spin con-

 0734-2101/87/053171-04$01.00

centrations, with uncertainties of about 25%–50%.

The $Hg_{1-x}Cd_xTe$ samples used in the EPR experiments were nominally undoped bulk single crystals with volumes between 10 and 50 mm^3. The semi-insulating (SI) CdTe crystals had been purchased from II–VI, Inc. The *p*-type $Hg_{0.7}Cd_{0.3}Te$ crystals were obtained from Cominco and New England Research Corporation (NERC). While the orientations for the major faces were known in some cases, several $Hg_{0.7}Cd_{0.3}Te$ wafers had been sliced at random. Some properties of the crystals that were subsequently boron implanted are presented in Table I. EPR measurements were performed on all the $Hg_{1-x}Cd_xTe$ materials prior to implantation. One of the CdTe crystals (i.e., sample C1) gave EPR spectra that correspond to the paramagnetic transition metals Fe^{+3} and Co^{+2} previously seen by others.[8] No EPR signals have been observed from any of the other $Hg_{1-x}Cd_xTe$ samples listed in Table I. When these crystals were cooled to temperatures below 15 K, *in situ* illumination with UV-filtered, IR-filtered, and an unfiltered 250-W xenon lamp had no noticeable effect upon the EPR signals for any $Hg_{1-x}Cd_xTe$ sample. In particular, there was no evidence for the $g \approx 2.35$–2.5 or $g = 3.0$ paramagnetic centers recently reported for undoped *p*-type $Hg_{0.7}Cd_{0.3}Te$ by Jones *et al.*[13] It should be noted that the acceptor levels for the $Hg_{0.7}Cd_{0.3}Te$ crystals in Table I vary by more than a factor of 6. Although numerous experimental factors can preclude[4,16] the observation of EPR spectra, considerable efforts were made to alter the present operating conditions so that paramagnetic signals could be detected. Some cavity tuning and stability difficulties were encountered with the narrower band gap $Hg_{0.7}Cd_{0.3}Te$ samples even before the ion implants, which generate highly conductive surface layers that lead to well-known[16] skin-depth effects. However, any significant concentrations of paramagnetic centers would have been detected if they had been present.

The boron($^{11}B^+$) ions were implanted into the $Hg_{1-x}Cd_xTe$ samples with a model 400 MPR-Veeco/AI ion-implanter system. The implants were done at room temperature with low ion dose rates to minimize inadvertent heating effects. No new EPR signals were observed from various $Hg_{1-x}Cd_xTe$ crystals for boron implants with energies from 40 to 250 keV and total doses up to 2×10^{15} ions/cm^2. Since thresholds for the observations of implant-induced EPR spectra had been reported for other semiconductors,[14,15] a heavy four-stage implant (i.e., 2.5×10^{15} B^+ ions/cm^2 at 100, 200, 300, and 400 keV) was done to produce a total dose of 1×10^{16} B^+ ions/cm^2. Samples from all of the crystals in Table I were simultaneously implanted under these conditions, which are expected[17] to produce a fairly uniform (although the mean boron content will decrease with distance from the implant surface) ^{11}B distribution more than 1 μm into the $Hg_{1-x}Cd_xTe$ crystals. The actual *n*–*p* junction will probably lie deeper,[18] but its position has not been determined. The present intent was to produce sufficiently large volumes of boron implant and damage regions to facilitate detection of any paramagnetic centers with the available EPR equipment.

TABLE I. Properties of $Hg_{1-x}Cd_xTe$ samples used for boron implantation studies, where composition (x) is given in the second column.

I.D. label	x	Implant face	Crystal source	Type	Carrier contents[a] (10^{15} cm^{-3})	Paramagnetic species seen before implants
C1	1.00	⟨111⟩	II–VI, Inc.	SI[b]	···	Fe^{+3},Co^{+2}
C3	1.00	⟨100⟩	II–VI, Inc.	SI	···	None
H5	0.32	⟨110⟩	Cominco	*p*	9	None
H6	0.32	⟨110⟩	Cominco	*p*	60	None
H7	0.31	Random	NERC	*p*	13	None

[a] From 77 K Hall data provided by the vendors.

[b] SI denotes semi-insulating (i.e., resistivity $> 10^6$ Ω cm at room temperature).

III. EFFECTS OF BORON ION IMPLANTS

After room-temperature $^{11}B^+$ implants with four energies to a total dose of 1×10^{16} ions/cm^2, new EPR spectra were observed from the $Hg_{1-x}Cd_xTe$ samples listed in Table I. Figure 1 shows a representative first-derivative spectrum for an implanted $Hg_{0.7}Cd_{0.3}Te$ crystal when it was cooled to 5 K. Similar signals were obtained between 2 and 78 K although cavity tuning became more difficult at higher temperatures. As illustrated in Fig. 1, Lorentzian line shapes give much better fits to experimental traces obtained at 5 K or higher temperatures than Gaussian curves. Very similar results have been found for the implant-induced signals from the other implanted $Hg_{1-x}Cd_xTe$ samples. In several cases, significantly improved fits occurred by including a second Lorentzian line with a narrower width. It is possible that inhomogeneous distributions of the paramagnetic centers created during implantation are responsible. The *g*-factor constants, peak-to-peak linewidths (ΔH_{pp}), and the paramagnetic spin concentrations normalized to sample weights that were derived from the fitted EPR spectra are summarized in Table II. The actual densities of paramagnetic centers are much greater than indicated in Table II since the defects are presumably confined to regions affected by the boron implants which only penetrate 1 μm or so into the crystals.

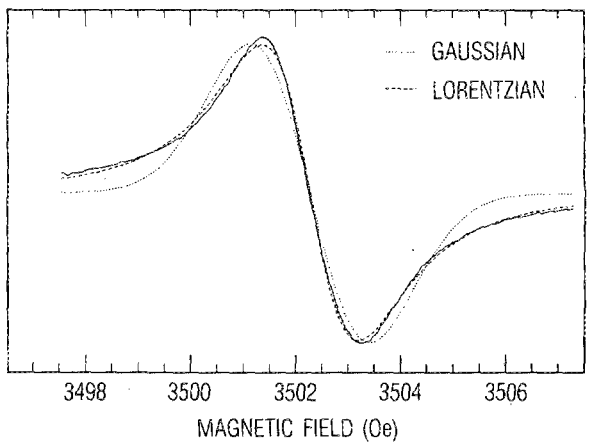

FIG. 1. Comparison of Lorentzian and Gaussian least-squares fits to the EPR derivative line shape obtained at 4 K from the $^{11}B^+$ implanted $Hg_{0.68}Cd_{0.32}Te$ sample (H6) when the magnetic field is along the ⟨110⟩ direction.

TABLE II. Summary of EPR parameters for $^{11}B^+$ ion implanted $Hg_{1-x}Cd_xTe$ crystals where the total dose was 1×10^{16} ions/cm^2 and T corresponds to the temperature during the EPR measurements. Magnetic fields approximately perpendicular to implanted crystal face for each sample.

Sample label	x	T (K)	Annealing conditions	g factor	ΔH_{pp} (G)	Nominal concentration (spins/g)
C1	1.00	5	As implanted	2.0030(1)	6.7	2.3×10^{14}
				2.0028(1)	2.6	0.3×10^{14}
C3	1.00	5	As implanted	2.0028(1)	6.8	5.9×10^{14}
H5	0.32	2	As implanted	2.0028(2)	3.5	···
		2	200 °C, 1 h	2.0028(1)	2.5	···
		2	300 °C, 1 h	2.0029(1)	4.6	4.0×10^{14}
				2.0023(1)	1.7	1.1×10^{14}
H6	0.32	4	As implanted	2.0028(1)	1.8	3.5×10^{15}
H7	0.31	5	As implanted	2.0029(1)	6.0	6.7×10^{14}
				2.0028(1)	2.4	0.4×10^{14}

Unfortunately, the dimensions of the damaged regions are not currently known. However, the effective densities are probably between 10^{17} to 10^{19} spins/cm^3 if the paramagnetic defects are assumed to be distributed from 1.0 to 10 μm below the surface.

The g-factor constants in Table II are considered equivalent for all the implanted $Hg_{1-x}Cd_xTe$ samples and are also nearly identical to the free-electron g factor (g_e) of 2.0023. Although these g factors are very slightly anisotropic, a positive g-factor shift (i.e., $g-g_e$) of $5(1)\times10^{-4}$ has been obtained. Ion implants have previously produced paramagnetic "dangling-bond" defects in Si (Ref. 14) and GaP (Ref. 15) with isotropic g factors of 2.0059 and 2.0032, respectively. These dangling-bond centers are usually attributed[19] to localized electronic states formed when covalent bonds are broken. Although the character of a dangling-bond defect in an ionic II–VI semiconductor such as CdTe is not obvious, the g factors in Table II for boron-implanted $Hg_{1-x}Cd_xTe$ are consistent with these defects. In contrast, the g factors for boron-implanted CdTe samples are distinctly different from the $g\approx1.7$ reported by others[9] for shallow donor states in chemically doped CdTe. Low-temperature (i.e., ~10 K) illuminations of all the boron-implanted $Hg_{1-x}Cd_xTe$ crystals also did not generate $g\approx1.7$ EPR signals associated with shallow donors. Furthermore, the measured temperature dependencies of the EPR intensities for boron-implanted $Hg_{1-x}Cd_xTe$ samples exhibit an inverse temperature behavior expected for isolated unpaired spins rather than the temperature-independent intensities found[16] for conduction electrons. Hence, the EPR spectra produced by boron implants do not directly correspond to the degenerate conduction bands commonly seen [1–3] in implanted HgCdTe. While deep donors usually give[20] small shifts in g factors, they also give rise to hyperfine splittings as noted previously[10,11] in doped CdTe. Isolated boron deep donor states should produce distinctive hyperfine patterns for both the ^{10}B and ^{11}B isotopes. However, the EPR spectra for boron-implanted $Hg_{1-x}Cd_xTe$ do not give any indication of these hyperfine splittings. Of course, electron spin-exchange effects[4]

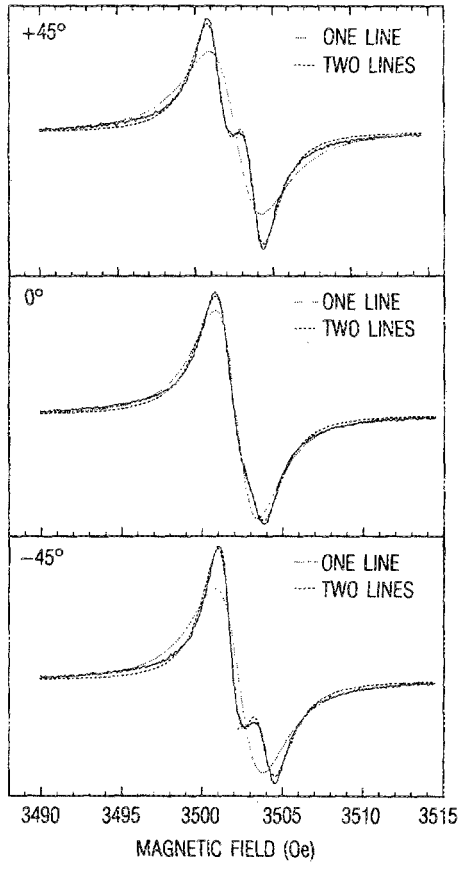

FIG. 2. Changes in the 2 K EPR derivative line shapes as the $^{11}B^+$ implanted $Hg_{0.68}Cd_{0.32}Te$ crystal is rotated $\pm$ 45° in unspecified directions from the ⟨110⟩ axis.

between closely spaced paramagnetic centers as well as rapid hopping motions of the spins[20] can eliminate these splittings and produce unsplit and narrowed Lorentzian lines as are observed from the implanted crystals. In fact, the smallest ΔH_{pp} value occurs for the H6 sample with the largest concentration of these paramagnetic centers, which is consistent with the electron spin exchange mechanism.

When the $^{11}B^+$ implanted $Hg_{09.7}Cd_{0.3}Te$ crystals are cooled below about 4 K, partially resolved two-component line shapes are observed for some orientations as shown in Fig. 2. Although these anisotropic line shapes could be caused by hyperfine interactions, they cannot be readily interpreted from the natural distribution of the Hg, Cd, or Te isotopes or the expected quadruplet for an isolated ^{11}B center. Consequently, the two EPR components that are clearly seen in Fig. 2 probably arise from two (or more) independent defect centers with slightly different g factors. Figure 3 illustrates the collapse of the two-component line for the implanted $Hg_{0.68}Cd_{0.32}Te$ sample H6 into a single peak as the temperature is raised. A symmetric and nearly Lorentzian line shape is found above 6 K where ΔH_{pp} values systematically decrease from 1.7 to 1.2 G as the temperature increases to 30 K. This behavior for ΔH_{pp} could be caused by a thermally activated process where the paramagnetic spins hop between inequivalent locations. While the identities of these defects cannot be established from the available data,

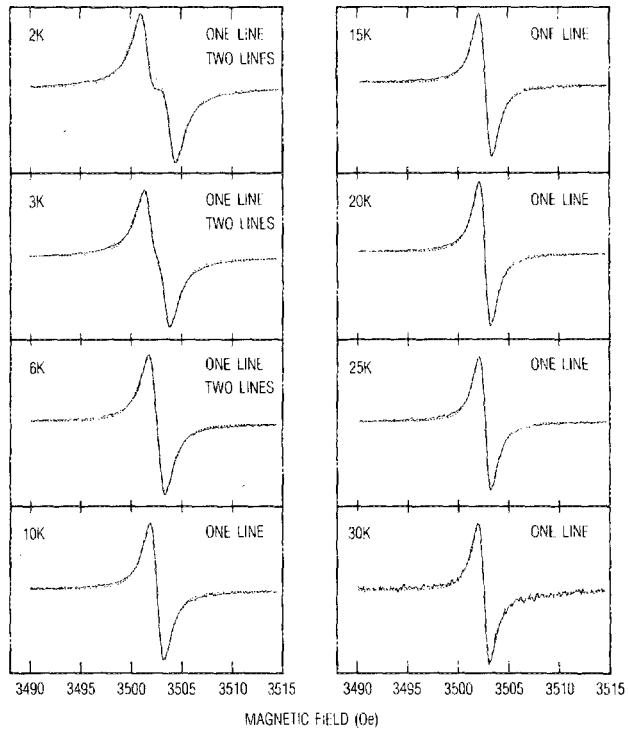

FIG. 3. Comparisons of two-line and one-line fits to $+45°$ orientation of implanted $Hg_{0.68}Cd_{0.32}Te$ sample at different temperatures. For temperatures above 6 K, the two-line fits cannot be distinguished from the one-line fits and are not shown.

closely spaced but independent centers would be required. Similar changes in the low-temperature line shapes were observed from the other implanted $Hg_{1-x}Cd_xTe$ samples although the linewidths were generally too large to give the resolutions shown in Figs. 2 and 3. Furthermore, the simultaneous presence of broad and narrow lines obscured these anisotropic line-shape separations for some samples. However, the ΔH_{pp} reduction with increasing temperature is reproduced by all implanted samples.

Studies of thermal anneals on the EPR spectra generated by the $^{11}B^+$ implants have been initiated. One-hour anneals up to 300 °C do not cause significant changes in the g factors or signal intensities. However, as indicated in Table II some changes in line shapes and ΔH_{pp} values are noted after these anneals. Since only minor alterations in the paramagnetic defect distributions were produced by these anneals, which are known[1-3,13,18] to remove various defects from implanted $Hg_{1-x}Cd_xTe$, the behavior of the EPR signals do not appear to be related to these particular defects. Further experiments that evaluate $^{10}B^+$ implants at different conditions and doses as well as more varied anneals are in progress to help establish the microscopic identities of the paramagnetic centers created in $Hg_{1-x}Cd_xTe$ by boron implants. These results will be reported elsewhere.

ACKNOWLEDGMENTS

We wish to thank Professor S. I. Chan for making available the EPR spectrometer at Caltech, R. E. Robertson for assistance with the samples, and Dr. J. F. Knudsen for the ion implants. The work at The Aerospace Corporation has been supported by the U. S. Air Force Space Division under Contract No. F04701-85-C-0086. Sandia National Laboratories are operated for the U. S. Department of Energy under Contract No. DE-AC04-76DP00789.

[1] M. B. Reine, A. K. Sood, and T. J. Tredwell, in *Semiconductors and Semimetals*, edited by R. K. Willardson and A. C. Beer (Academic, New York, 1981), Vol. 18, p. 201.
[2] G. L. Destefanis, Nucl. Instrum. Methods **209/210**, 567 (1983).
[3] T. W. Sigmon, Nucl. Instrum. Methods B **7/8**, 402 (1985).
[4] J. E. Wertz and J. R. Bolton, *Electron Spin Resonance-Elementary Theory and Practical Applications* (McGraw-Hill, New York, 1972).
[5] R. S. Title, in *Physics and Chemistry of II–VI Compounds*, edited by M. Aven and J. S. Prener (American Elsevier, New York, 1967), p. 265.
[6] J. Schneider, in *II–VI Semiconducting Compounds*, edited by D. G. Thomas (Benjamin, New York, 1967), p. 40.
[7] J. W. Corbett, R. L. Kleinhenz, and N. D. Wilsey, in *Defects in Semiconductors*, edited by J. Narayan and T. Y. Tan (North-Holland, New York, 1981), p. 1.
[8] A. Zunger, Solid State Phys. **39**, 275 (1986).
[9] K. Saminadayar, D. Galland, and E. Molva, Solid State Commun. **49**, 627 (1984); K. Saminadayar, J. M. Francou, and J. L. Pautrat, J. Cryst. Growth **72**, 236 (1985).
[10] R. C. DuVarney and A. K. Garrison, Phys. Rev. B **12**, 10 (1975).
[11] G. Brunthaler, W. Jantsch, U. Kaufmann, and J. Schneider, Phys. Rev. B **31**, 1239 (1985).
[12] A. K. Koh, D. J. Miller, and C. T. Grainger, Phys. Rev. B **29**, 4904 (1984).
[13] C. E. Jones, K. James, J. Merz, R. Braunstein, M. Burd, M. Eetemadi, S. Hutton, and J. Drumheller, J. Vac. Sci. Technol. A **3**, 131 (1985).
[14] B. L. Crowder, R. S. Title, M. H. Brodsky, and G. D. Pettit, Appl. Phys. Lett. **16**, 205 (1970); G. Gotz, W. Karthe, B. Schnabel, and N. Sobolev, Phys. Status Solidi A **50**, K209 (1978).
[15] T. Matsumori, K. Miyazaki, and S. Shigetomi, Appl. Phys. Lett. **42**, 521 (1983).
[16] R. S. Alger, *Electron Paramagnetic Resonance: Techniques and Applications* (Interscience, New York, 1968).
[17] H. Ryssel, K. Muller, J. Biersack, W. Kruger, G. Lang, and F. Jahnel, Phys. Status Solidi A **57**, 619 (1980).
[18] L. O. Bubulac, J. Cryst. Growth **72**, 478 (1985).
[19] M. H. Brodsky and R. S. Title, Phys. Rev. Lett. **23**, 581 (1969); P. A. Thomas, M. H. Brodsky, D. Kaplan, and D. Lepine, Phys. Rev. B **18**, 3059 (1978).
[20] C. Gonzalez, D. Block, R. T. Cox, and A. Herve, J. Cryst. Growth **59**, 357 (1982).